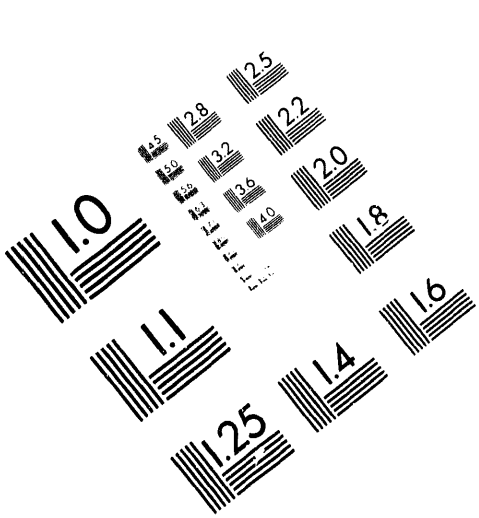

Association for Information and Image Management

1100 Wayne Avenue, Suite 1100
Silver Spring, Maryland 20910

301/587-8202

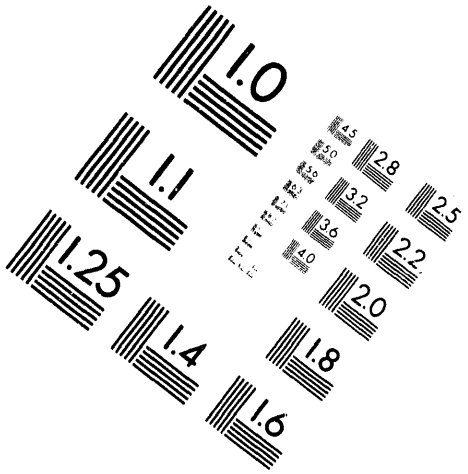

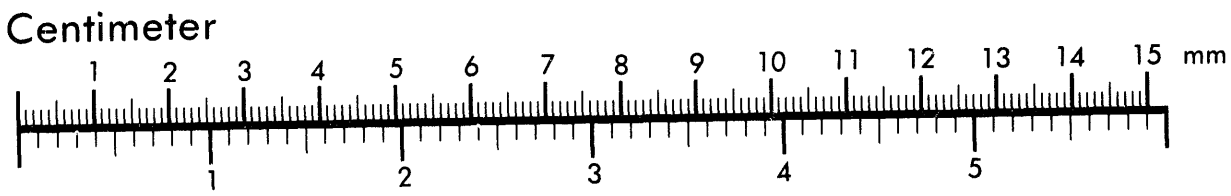

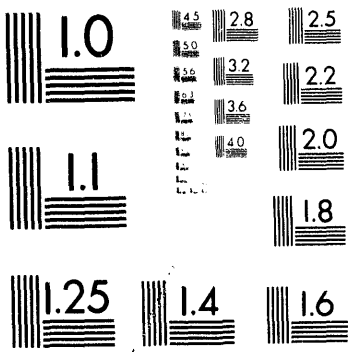

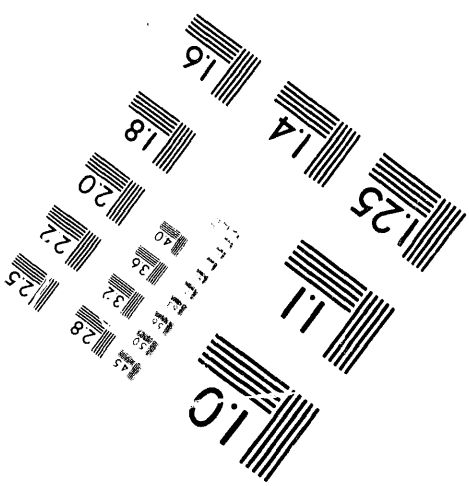

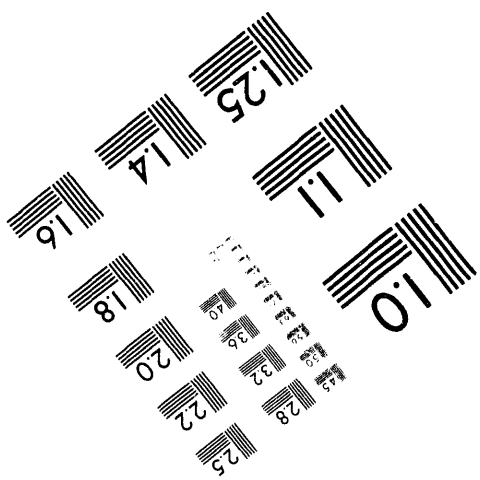

1 of 1

Conf-940978--3

SAND94-1674C

ION EMISSION INTENSITY RATIOS AS A FUNCTION OF ELECTRODE GAP, MELTING CURRENT, AND PRESSURE DURING LOW CURRENT VACUUM ARC REMELTING

Rodney L. Williamson
Sandia National Laboratories
Albuquerque, New Mexico 87185

S. M. Grose
Inco Alloys International, Inc.
Huntington, West Virginia 25720

Abstract

The arc energy distribution in the electrode gap plays a central role in the vacuum arc remelting (VAR) process. However, very little has been done to investigate the response of this important process variable to changes in process parameters. Emission spectroscopy was used to investigate variations in arc energy in the annulus of a VAR furnace during melting of 0.43 m diameter Alloy 718 electrode into 0.51 m diameter ingot. Time averaged (1 second) intensity data from various chromium atom and ion (Cr^+) emission lines were simultaneously collected and selected intensity ratios were subsequently used as arc energy indicators. These studies were carried out as a function of melting current, electrode gap, and CO partial pressure. The data were modeled and the ion electronic energy was found to be a function of electrode gap, the energy content of the ionic vapor decreasing with increasing gap length; the ion ratios were not found to be sensitive to pressure. On the other hand, the chromium atom electronic energy was difficult to model in the factor space investigated, but was determined to be sensitive to pressure. The difference in character of the chromium ion and atom energy fluctuations in the furnace annulus are attributed to the difference in the origins of these arc species and the non-equilibrium nature of the metal vapor arc. Most of the ion population is emitted directly from cathode spots, whereas much of the atomic vapor arises due to vaporization from the electrode and pool surfaces. Also, the positively charged ionic species interact more strongly with the electron gas than the neutral atomic species, the two distributions never equilibrating due to the low pressure.

This work performed at Sandia National Laboratories is supported by the United States Department of Energy under contract DE-AC04-94AL85000. The authors gratefully acknowledge the support and cooperation of Cytemp Specialty Steel, Inc., Titusville, Pennsylvania, as well as that of the Specialty Metals Processing Consortium.

Introduction

Vacuum arc remelting (VAR) is a re-melting process widely used throughout the specialty metals industry in the production of segregation sensitive and/or reactive metal alloys. The process involves striking an electrical arc between an electrode (cathode) consisting of the material to be re-melted and the bottom of a cylindrically shaped, water cooled, copper crucible (anode). Heat from the arc causes material at the electrode tip to melt and drip into the crucible forming a molten pool. As the process progresses, a semi-directionally solidified ingot forms with a molten pool situated on top. Because the electrode is of smaller diameter than the crucible, it must be driven down to maintain a constant gap between the electrode tip and the molten ingot top as the ingot grows. The gap between the pool surface and average electrode tip position is known as the electrode gap (G). It is important for the success of the process that the solidification front reach a steady-state condition and not be significantly perturbed during a melt. This assures that the product will be free of solidification defects brought on by instabilities in the liquid-solid interface region (the mushy zone). The underlying assumption of current VAR control practice is that steady-state melting conditions are met by holding the melting current (I), electrode gap, ingot cooling gas (if used) and ambient furnace pressure constant. However, no effort is made to monitor the arcing conditions in the furnace to determine if these measures are adequate.

Traditionally, the only available measure of change in arcing conditions during VAR has been average arc voltage. While it is true that arc voltage is an indicator of arcing conditions, the relation between arcing conditions in the VAR process and voltage is not straightforward. One can easily envision a situation where the arc is localized on a small, non-central part of the electrode with no clearly distinguishable voltage characteristic relative to the case where the arc is evenly distributed across the entire electrode face. Such a situation would clearly be undesirable since prolonged localized energy input to the ingot would severely disrupt the solidification process and give rise to solidification defects as well as adversely affect ingot surface quality. Hence, it is important to find more sensitive measures of arcing conditions if one is to more fully characterize the VAR process. Once characterized, the new understanding may be applied to the task of process diagnosis and control optimization.

One potential measure of arcing behavior is the emission spectral energy distribution, i.e. how the electronic energy is distributed among the energy levels of the ensemble of emissive excited-state atoms and ions in the arcing region. The integrated area under an emission line for a particular arc component is proportional to the number density of that particular excited state component. The proportionality constant is given by $g_n A_{nm}$, where g_n is the degeneracy of state n and A_{nm} is the emission probability coefficient (Einstein coefficient) describing the probability that the system will relax from state n to state m through emission of a photon of energy E_{nm}. Hence, the ratio of two emission line areas from a particular arc component is proportional to the population of that component in one energy state relative to the other energy state. Given that one energy state will be higher than the other, this ratio will comprise an indicator of the electronic energy content of that arc component. Under conditions of thermodynamic equilibrium, or at least local thermodynamic equilibrium (LTE), where the energy distributions for the arc components conform to Boltzmann statistics, the ratio would be an indicator of arc temperature. Such conditions are not met in the VAR plasma. However, earlier work has demonstrated that the individual ion and atom energy distributions in a VAR arc are Boltzmann-like, and that a meaningful effective "temperature" for each arc component may be calculated.[1] Hence, the following relationship holds:

$$\frac{I_{nm}}{I_{pq}} = \frac{g_p A_{pq} \lambda_{nm}}{g_n A_{nm} \lambda_{pq}} e^{-E_{np}/kT_{eff}} \qquad (1)$$

where λ_{nm} is the wavelength of the n-m transition and "I" is understood as emission intensity and not arc current. Thus, fluctuations in the intensity ratio should indicate fluctuations in T_{eff} for the arc component under investigation which, in turn, should be an indicator of arc condition. The intent is this experiment is not to calculate T_{eff} for the various arc components but to characterize how the ratios for two major arc plasma components, Cr and Cr^+, behave as a function of the parameters I, G, and P.

In this experiment, changes were induced in the furnace arc by varying melting current, electrode gap, ambient pressure, or some combination of these. Changes in arcing conditions were monitored by observing and recording the spectral content of the light emitted through the viewing port of the furnace so as to be able to determine fluctuations in the spectral energy of the arc. These data were analyzed and statistical models of the response to changes in the three independent variables were constructed. In this paper, the experiment is described, pertinent features of the statistical models are discussed, and a determination is made as to whether this response has diagnostic or process control value.

Experimental Procedures

Figure 1 shows the factor space design used in the Cytemp experiment. Melting current was varied from 5 to 10 kA, electrode gap from 6 to 51 mm, and ambient furnace pressure (P) from 10 to 100 mm. The data were collected during a single heat while melting a 0.43 m diameter Alloy 718 electrode into a 0.51 m diameter ingot. Furnace pressure was controlled through the addition of carbon monoxide. The order of the factor space points is indicated in Figure 1 by the number accompanying each point. Before the beginning of a trial, the furnace was stabilized at the specified conditions of the factor space point; this usually required ~30 minutes. Each trial consisted of a ~10 minute period during which data were collected. The gap was checked at the beginning and end of each trial as described below. Table I shows the measured values of electrode gap, melting current and furnace ambient pressure actually obtained at each point in the factor space experiment depicted in Figure 1.

During each trial, melting current, pressure data and an absolute time signal were continuously acquired and stored on an analog tape recorder (Honeywell Model 101) for later play-back and analysis. The bandpass of the tape recorder at the tape speed used (15 ips) was 10 kHz. Melting current data were acquired from a Hall-effect transducer (Halmar Model 7ADM) mounted on the furnace power supply bus bar. The output of this device is a voltage that is directly proportional to the current (10 mV/kA). The transducer's signal was amplified and fed into one of the tape recorder inputs. Ambient furnace pressure was measured using a capacitance manometer type transducer (Baratron Model 227HS-A-1); the voltage output from this transducer is directly proportional to the pressure. Finally, an absolute time signal was recorded on the tape using a time code generator (Datum, Inc., Model 9300).

At the beginning and end of a trial, the electrode gap was checked. This was accomplished by manually driving the electrode down until a non-transient arc interruption caused the ram scram circuit to energize and rapidly withdraw the electrode. A computer (DEC LSI-11)

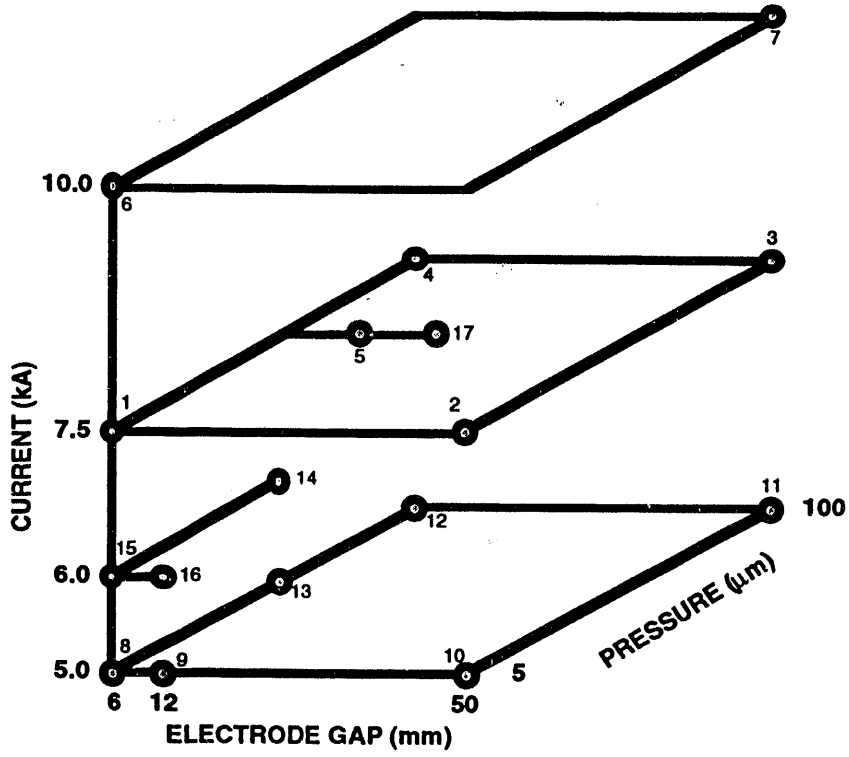

Figure 1 - A map of the factor space design used in this experiment. Each data collection point is labeled in the order of the experiment.

Table I Measured values of electrode gap, melting current and pressure used at each point in the factor space experiment depicted in Figure 1.

TRIAL NO.	G (mm)	I (kA)	P (mm)
1	5.5	8.2	3
2	46.7	7.9	4
3	38.9	7.9	109
4	6.0	7.6	108
5	20.2	7.5	56
6	6.3	9.9	7
7	35.7	11.2	108
8	5.7	5.2	5
9	10.9	5.3	3
10	42.6	5.1	4
11	55.8	5.0	110
12	9.0	5.0	103
13	7.8	5.1	58
14	4.1	6.2	58
15	3.6	6.4	6
16	10.4	6.4	4
17	12.4	8.1	52

was used to acquire data during the gap check. Arc voltage was read directly into the computer over an analog-to-digital converter. Simultaneously, ram position data were acquired using a linear displacement transducer (Temposonics II, MTS Systems Corp.). This device outputs a 17 bit parallel signal that is read by the computer. The gap was determined by noting the point on the ram position trace where the electrode touched the pool surface as indicated by a rapid decrease in voltage. This position measurement was subtracted from the ram position measured before the gap check was started, the difference defining the electrode gap.

Furnace pressure was controlled using a flow controller (MKS Model 250B) and valve arrangement. Data from the pressure gauge were input to the flow controller. The controller used these data to compare actual pressure with a pre-specified set-point; it then operated the valve to achieve the set-point pressure.

Figure 2 shows a schematic diagram of the viewing port modification and optics used in collecting furnace emissions. The stock viewing port mirror was replaced with a front surfaced, aluminized mirror, and the stock window was replaced with one constructed from UV-grade fused silica. These modifications were necessary to allow ultraviolet (UV) light to pass unattenuated out of the furnace; many ionic arc plasma species emit in the UV portion of the electromagnetic spectrum. Also shown in the figure is a slit plate. This plate was used in place of the normal shield glass which quickly becomes coated with metal dust, film and splatter. The slit admits light while mostly protecting the mirror from contamination. The collection lens was positioned so that the slit was located in its focal plane, causing the optical cable face to be imaged onto the slit. All light that passed through this image was collected and transported via the optical cable to the spectrometer optics. The optical cable used for these experiments is 1 m long and consists of a bundle of 1 mm diameter UV grade fused silica fibers.

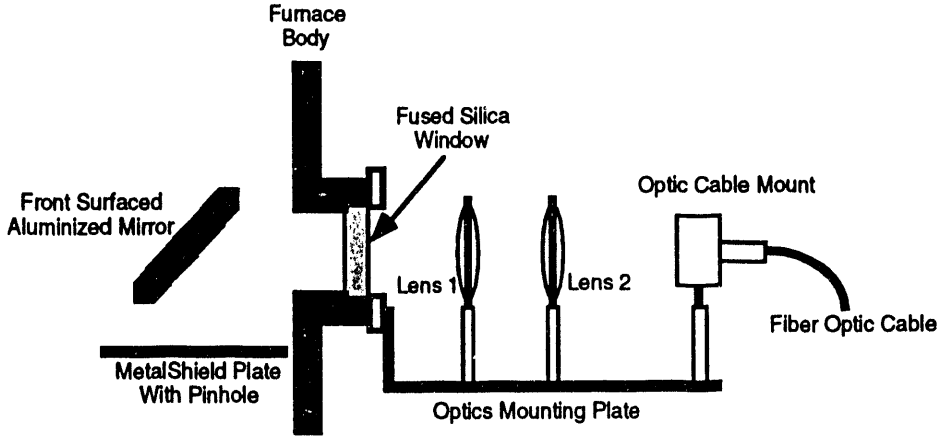

Figure 2 - Schematic diagram of the viewing port modification and optics used in the collection of arc emissions.

The spectral content of the furnace arc emissions was investigated using a 0.32 m focal length monochromator (ISA Model HR320) equipped with a 2,400 groove/mm holographic grating. Inside the spectrometer the light was spectrally dispersed into its component wavelengths and focused onto the photodiode array of an optical multi-channel

analyzer (OMA) detector head (Tracor Northern Model 6114). Once calibrated, the OMA system yields intensity vs wavelength data. Two computers (Compaq Model 386/25e) were used to control the experiment. One computer was used for timing and spectrometer scanning chores, and was equipped with a data acquisition card (National Instruments Model AT-MIO-16L) and an IEEE-488 parallel interface card (National Instruments Model AT-GPIB) to accomplish this. The second computer interfaced with the OMA controller (Tracor Northern Model TN6600) using hardware and software supplied by the OMA manufacturer.

Spectroscopic data at three different wavelengths were recorded at each point in the factor space. Spectra were acquired sequentially at wavelengths of 283.0, 303.0 and 395.0 nm. At each wavelength, ten consecutive emission spectra were acquired with a typical exposure time of 1.00 second. Subsequent to such an acquisition, the spectrometer wavelength was scanned to the next position and the process repeated until spectra had been acquired at all three wavelengths. The data were recorded on computer disk for later calibration and analysis. The spectrometer system was calibrated at Sandia subsequent to the Cytemp experiment using a calibrated radiance source (Optronic, Inc., Model IR-284) traceable to NIST.

One Cr and two Cr^+ ratios were investigated as indicators of arc energy content (T_{eff}): Cr - $I_{390.9}^{4.17}/I_{396.4}^{5.67}$, Cr^+ - $I_{284.3}^{5.88}/I_{281.8}^{8.55}$ and Cr^+ - $I_{312.0}^{6.41}/I_{298.9}^{7.89}$. The subscripts denote the wavelengths (in nm) of the emission lines that were integrated and the superscripts denote the energy (in eV) of the excited electronic state from which the emission originates. An increase in any of these ratios indicates a fall in the effective atom or ion electronic energy content since the lower energy state is placed in the numerator of each ratio. None of the emissive transitions selected for this study terminate in the ground electronic state, assuring that the plasma is optically thin at these wavelengths.

The data were modeled using multiple regression analysis. As a general rule, the data were initially fit using I, G, P and all second-order interaction terms (e.g. I^2, IG, etc.). All regression analysis was carried out on a Macintosh IIx computer (Apple Computer Inc.) using StatView™ statistical software (Abacus Concepts, Inc.).[2]

Data and Results

Spectral Survey

In this section, representative emission spectra are shown and the various lines identified. These spectra were acquired under conditions of intermediate current (7.9 kA), large electrode gap (46 mm) and low pressure (4 mm), corresponding to Trial 2 in the factor space. The large gap condition gives more intense spectra and, thus, better signal-to-noise ratios because the arc is more active on the electrode sides.

Figure 3 shows an emission spectrum acquired with the spectrometer set at 283.0 nm. The two most prominent features (off scale in the figure) of the spectrum are Mg^+ emission lines at 279.55 and 280.27 nm. Other major lines in this region are due to Mg (285.21 nm), Mn (279.83 and 280.10 nm), and Cr^+ (283.56, 284.33, and 284.98 nm). Note that because of the high volatility of manganese and especially magnesium, these elements are always strongly represented in the Alloy 718 arc spectrum even though they are present in the alloy only in very small quantities. Cr^+ lines account for most of the low intensity

output in this spectral region, but Fe^+, Mg and Mg^+ lines are also present. One of copper's stronger emission lines is located at 282.44 nm; its extreme weakness indicates that very little copper is in the arc. Conceivably one could use this emission line to determine if the arc were attached to the crucible rather than the ingot surface. The Cr^+ emission lines at 284.33 and 281.84 nm originate from excited electronic Cr^+ states with energies (relative to the ground state) of 5.88 and 8.55 eV, respectively, and terminate in states lying at energies of 1.53 and 4.16 eV, respectively.[3] These lines are used in the ion spectral energy studies described below.

Figure 4 shows the spectral region centered about 303.0 nm. There are prominent features due to Mn^+ at 293.31, 293.93 and 294.92 nm, however, the most numerous lines are due to Cr^+. The Cr^+ lines at 312.26 (very weak) and 298.92 nm originate from excited electronic states with energies of 6.41 and 7.89 eV, respectively, and terminate in electronic states with energies of 4.18 and 3.74 eV, respectively.[3] These lines were also used for the ion spectral energy studies described below. Other emission lines identified in this spectral region are due to Ni, Cr, Fe, Al, and Mg^+.

The dominant features of the spectral region centered about 395.0 nm are from Mn (403.08, 403.31 and 403.45 nm) and Ca^+ (393.37 and 396.85 nm), all of which are off scale in Figure 5. Fe, Ni, Cr, Mn and Al are present in this region. The Cr lines at 390.88 and 396.37 nm were used in the Cr spectral energy studies described below; they originate from excited states of Cr located at 4.17 and 5.67 eV above the ground state, respectively, and terminate in states lying at 1.00 and 2.54 eV, respectively.[3]

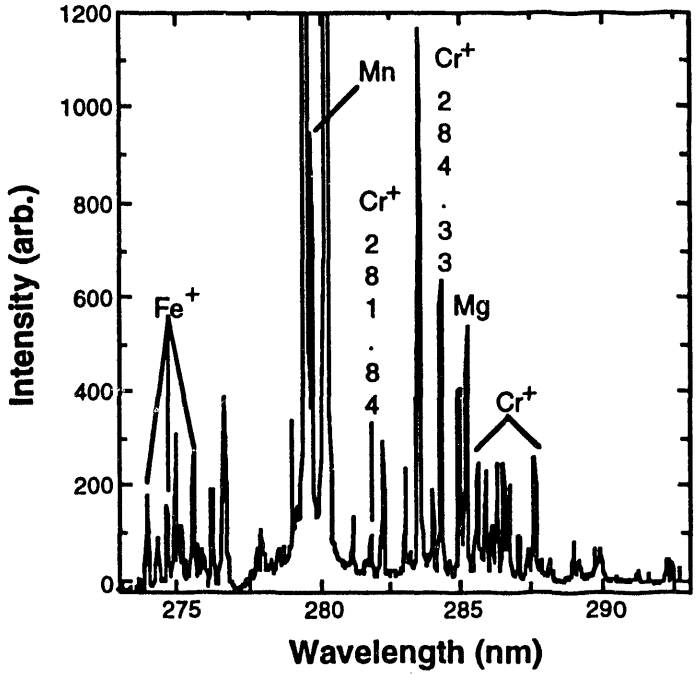

Figure 3 - Arc emission spectrum centered at 283.0 nm in the UV region of the spectrum.

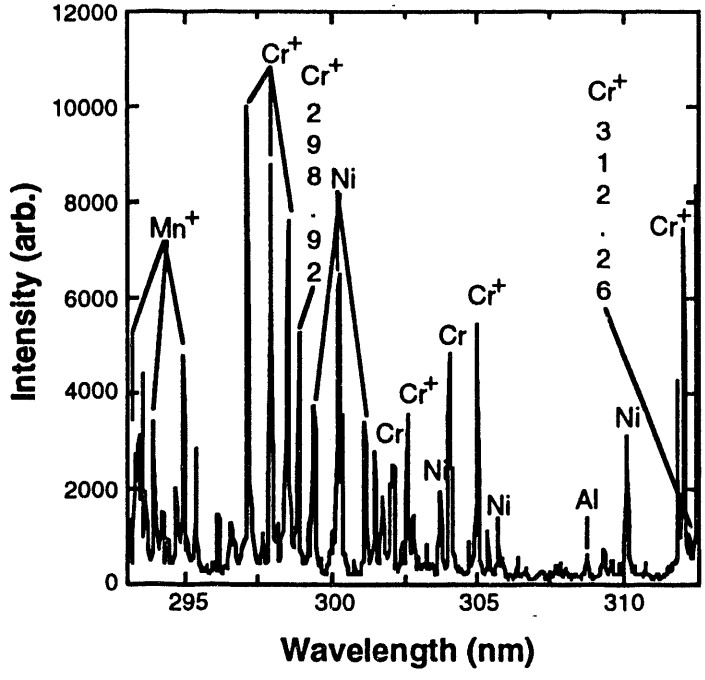

Figure 4 - Arc emission spectrum centered at a wavelength of 303.0 nm in the UV region of the spectrum.

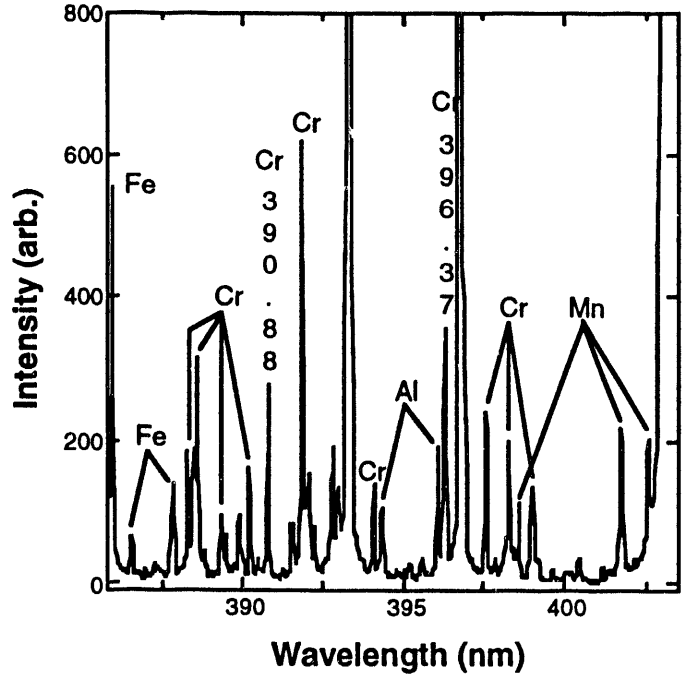

Figure 5 - Arc emission spectrum centered about 395 nm in the near-UV region of the spectrum.

Spectral Energy Studies

The chromium atom and ion ratio data are shown in Table II.

Table II Emission intensity ratio data.

TRIAL NO.	$I_{390.9}/I_{396.4}$	$I_{284.3}/I_{281.8}$	$I_{312.0}/I_{298.9}$
1	1.18	5.54	1.48
2	0.93	6.74	1.60
3	0.88	7.01	1.44
4	1.04	5.87	1.44
5	1.06	8.24	1.73
6	1.01	5.59	1.27
8	1.06	6.67	1.32
9	1.09	7.95	1.47
10	0.83	6.94	1.57
11	1.18	10.8	1.47
12	0.98	6.70	1.31
13	0.92	6.32	1.32
14	1.05	5.25	1.23
15	1.05	5.35	1.28
16	1.02	7.16	1.49
17	1.05	5.18	1.53

If the Cr^+ data sets are retained in their entirety, the responses of the two ratios may not be modeled satisfactorily, i.e. the models contain so many parameters that their physical significance is masked. The situation may be improved significantly by considering only a subset of the data, namely that data acquired at electrode gaps less than 25 mm.[4] When this is done, the responses may be modeled by the following equations.

$$I_{284/282} = 6.365 + 0.1816G - 0.2172I \pm 0.43 \quad (2)$$

$$I_{312/299} = 0.0612 + 0.02279G + 0.3198I - 0.02114I^2 \pm 0.06 \quad (3)$$

Eq.'s 2 and 3 account for approximately 86% and 88% of the variance in their respective responses, the standard error being given with each equation. Plots of the responses versus the fitted values as predicted by the models are shown in Figures 6 and 7. Neither model is particularly accurate; the error in gap prediction associated with the standard error in Eq.'s 2 and 3 is ±2.4 mm and ±2.6 mm, respectively. However, definite trends emerge from the models. First, in either case, the electrode gap alone accounts for approximately 75% of the variance in the response. Thus, for both data sets, the major driving force for the response of the Cr^+ energy content function is the change in electrode gap: as the gap is opened, T_{eff} decreases.[5] The second significant feature is that the models predict the response only at electrode gaps below ~25 mm. When the large (>35 mm) electrode gap data are included, significant additional variance is introduced. Furthermore, if only the high pressure data are deleted from the data sets, the situation is not improved. Hence, within the factor space investigated, P_{CO} does not play an important role in determining the ion "temperature" response.

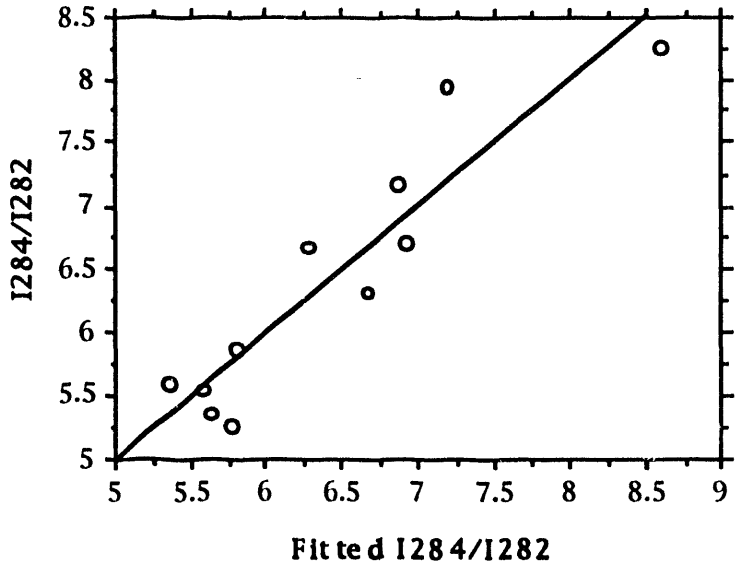

Figure 6 - Plot of the fit of Eq. 2 to the intensity ratio data.

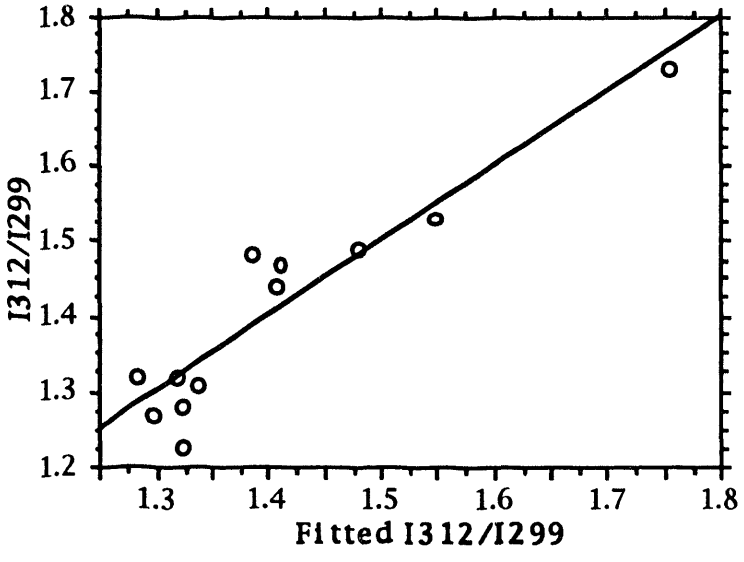

Figure 7 - Plot of the fit of Eq. 3 to the intensity ratio data.

The Cr atom ratio has a somewhat different character than the ion ratio. Inspection of the correlation matrix shows that no single parameter in the factor space can account for more than about 10% of the response, indicating that the neutral atom ratio is not strongly coupled to the chosen parameter set. Unlike the ion emission ratio case, removing the large electrode gap values from the data set does not help the situation. If, however, the highest pressure data (>100 mm CO) are removed, the situation improves somewhat. The remaining 12 data points may be fit using the following four parameter model which accounts for 89% of the variance:

$$I_{391/396} = 1.286 - 0.00543G - 0.05764P + 0.00219IP + 0.00070P^2 \pm 0.037 \quad (4)$$

The fit for this model is shown in Figure 8, and the standard error is included in the equation. It was evident from the standardized regression coefficients that the pressure terms play the major role in determining the response. However, these terms are highly correlated and none of them are well correlated to the response independently. Hence, the physical role of P remains ambiguous. The most highly correlated term is G, though it can only account for ~45% of the response independently.

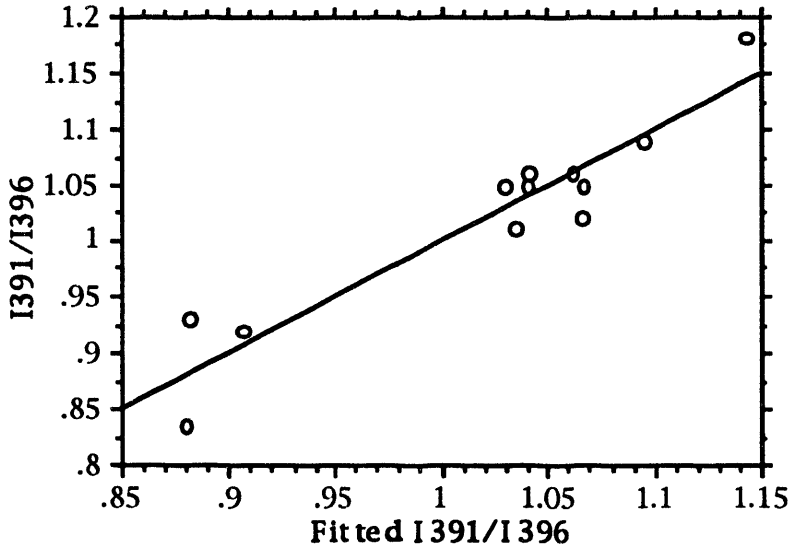

Figure 8 - Plot of the fit of Eq. 4 to the intensity ratio data.

Discussion of Results

As was shown above, the effective temperature of the ion distribution decreases linearly with increasing electrode gap. Assuming that the total number of ions and electrons in the gap region remains constant as the electrode gap is increased, the plasma density will decrease due to the increase in volume of the gap region. This decrease in overall plasma density leads to an increase in mean free path for electron-ion collisions and, hence, serves to weaken the coupling between the two populations. Because the electron gas is the heat source for the ions, the weaker electron/ion coupling gives rise to a decrease in the effective temperature of the ion distribution.[6] The assumption that the total ion and electron count remains constant at constant melting current as the gap is opened is valid only so long as the electrode gap changes are small relative to the characteristic length scale of the system, i.e. the electrode diameter. Under this condition, changes in electrode gap do not affect the energy flux partitioning between the ingot pool and the crucible wall. Hence, the particle flux from the surfaces into the gap region remains constant because the energy flux to the surfaces remains constant. If, however, a change in electrode gap is sufficiently large to significantly perturb the energy flux partitioning to the surfaces, another degree of freedom

is introduced which is poorly characterized. The data presented here indicate that this criterion is exceeded at an electrode gap value between 25 and 35 mm, since beyond this point the ion ratio response becomes poorly correlated to electrode gap.

The same type of argument predicts that the ion ratio should decrease (effective temperature increase) with increasing melting current. That is, as the melting current is increased, the energy flux to the surfaces increases. This should give rise to a higher plasma density in the electrode gap and a concomitantly enhanced electron/ion coupling. This trend is indicated by the melting current response of I_{284}/I_{282}, but the behavior of I_{312}/I_{299} exhibits this behavior only at melting currents greater than 7-8 kA. Unfortunately, the ion ratio response is rather flat over the melting current range investigated and the noise in the data is such that this ambiguity cannot be resolved. Therefore, it is concluded that the ion ratio response is not particularly sensitive to melting current under conditions typically used to produce 0.5 m Alloy 718 ingots.

Because the ion ratio response is sensitive to electrode gap, the possibility exists that it can be used as an electrode gap control response if the accuracy and signal processing time could be sufficiently enhanced. Such a device might find application under low current conditions where neither drip-short nor voltage control are applicable, such as during hot-topping, or as a check on existing gap measuring strategies. Though the method used to collect the spectroscopic data and accurately calculate the ratios was rather involved and time consuming in this experiment, hardware could be constructed that was dedicated to directly acquiring the ratio of interest. This and noise reduction techniques are topics of continued research.

As noted above, the chromium atom intensity ratio is not highly correlated to any particular parameter in the space. There are good reasons why it should not be similar in character to the ion ratio response. First, because the atoms are not electrically charged as are the ions, the cross-section for electron impact will be smaller.[7] Secondly, the majority of the excited-state neutral chromium atom density is associated with vaporization from surfaces [8], whereas the excited-state ion density comes from at least two primary sources: ionization of neutral atom vapor and cathode spot emission. Hence, it is not surprising that the excited-state population distributions for Cr and Cr^+ are not strongly coupled, and this has been observed experimentally.[1] The data further indicate that the Cr intensity ratio is very sensitive, though uncorrelated, to pressure. This is probably related to the observation that an oxide layer forms on the ingot pool surface when CO is added to the furnace.[9] Such a coating not only serves to perturb current collection and, hence, energy flux at the anode, but also inhibits vaporization of atomic species from the surface. It is likely that other correlations of this response (e.g. to electrode gap or melting current) are masked by this effect. Further investigation in the absence of CO pressure effects is warranted.

Conclusions

Chromium ion intensity ratios are sensitive functions of electrode gap up to values of ~25 mm, indicating that energy flux partitioning between the molten pool and crucible wall changes with changing gap beyond this point. Models of the ion ratio response demonstrate that the effective arc temperature decreases with increasing electrode gap. The models may be used to make electrode gap predictions to an accuracy of approximately ±2.5 mm under the conditions of this experiment. Dependence of the response on melting current was not adequately characterized. Such a response could be useful for control

under low melting current conditions, such as hot-topping, where drip-short and voltage control methods are not applicable. This assumes that noise reduction techniques can be developed to enhance the accuracy of the models and that a device may be constructed to characterize the response in a timely fashion.

The chromium atom intensity ratio studied indicated that this response was very sensitive, but uncorrelated, to CO partial pressure. Further studies of this response are necessary to determine its relationship to electrode gap and pressure.

References and Notes

1. R. L. Williamson et al., "Plasma Studies in a Vacuum Arc Remelting Furnace," in Plasma Processing and Synthesis of Materials (MRS Symposium Proceedings Vol. 98), ed. D. Apelian and J. Szekely, Materials Research Society (1987).

2. For more information on the general methods of regression analysis and model selection procedures, the reader is referred to the following text: N. Draper, and H. Smith, Applied Regression Analysis, Second Edition, Wiley, New York (1981).

3. S. M. Younger et al., "Atomic Transition Probabilities for Vanadium, Chromium, and Manganese (A Critical Data Compilation of Allowed Lines," J. Phys. Chem. Ref. Data, **7(2)** (1978).

4. In deriving Eq. 2, an additional point was deleted, namely the point at high current (8.1 kA), medium P_{CO} (52 mTorr), and medium electrode gap (12.4 mm). No justification for this is given other than the fact that its ratio is clearly anomalous. The value of R^2 is changed from 0.85 to 0.69 with this point included in the data set.

5. The role of melting current in determining T_{eff} for Cr^+ remains ambiguous. It enters Eq.s 2 and 3 in different ways, and in the case of Eq. 3, neither I nor I^2 make a significant independent contribution to the model.

6. E. Pfender, "Electric Arcs and Arc Gas Heaters," in Gaseous Electronics, Vol. 1: Electrical Discharges, M. N. Hirsh and H. J. Oskam, ed's, Academic Press, Orlando (1978) p. 302.

7. See, for example, I. I. Sobelman, L. A. Vainshtein and E. A. Yukov, Excitation of Atoms and Broadening of Spectral Lines, Springer-Verlag, Berlin (1981) pp. 120-1.

8. For evidence that the atom and ion densities are non-uniform in the electrode gap region, see R. L. Williamson, F. J. Zanner and W. A. Hareland, "Monochromatic Imaging Studies Of A Low Pressure Arc Burning On Molten Inconel 718 Electrodes During Vacuum Arc Remelting," in Special Melting and Processing Technologies, G. K. Bhat, ed., Noyes Publications, Park Ridge, New Jersey (1989) p. 496.

9. R. L. Williamson and F. J. Zanner, "Voltage Signatures in VAR," Proceedings of the 1991 Vacuum Metallurgy Conference on Melting and Processing of Specialty Materials, N. Bhat, E. W. Bloore and D. R. Malley, ed's, Iron and Steel Society, Warrendale, Pennsylvania (1992) pp. 87-91.

DISCLAIMER

DATE
FILMED
10/24/94
END